

# Site characterization of the INGV station IV.ROM9 - ROMA (INGV garden)

Working Group:  <b>Giuseppe DI GIULIO</b> <b>Maurizio VASSALLO</b> <b>Paola BORDONI</b> <b>Giovanna CULTRERA</b> <b>Giuliano MILANA</b> <b>Sara AMOROSO</b> <b>Daniela FAMIANI</b> <b>Fabrizio CARA</b> <b>Giorgia CARLUCCI</b> <b>Doriana ATTOLICO</b>	Date: March 2017
Subject: <b>Final report illustrating measurements, analysis and results at IV.ROM9 station</b>	

1	
<b>1. Introduction.....</b>	<b>3</b>
2	
<b>2. Geophysical investigation.....</b>	<b>4</b>
<b>2.1 Array Measurements Results .....</b>	<b>5</b>
3	
<b>3. Vs Model.....</b>	<b>10</b>
4	
<b>4. Conclusions.....</b>	<b>13</b>
<b>Disclaimer and limits of use of information.....</b>	<b>14</b>
<b>Esclusione di responsabilità e limiti di uso delle informazioni.....</b>	<b>15</b>

## 1. Introduction

In this report, we present the geophysical measurements and the results obtained in the framework of the 2016 agreement between INGV and DPC, named “*Allegato B2: Obiettivo 1 (Responsabile: C. Meletti) - TASK B: Caratterizzazione siti accelerometrici (Responsabili: P. Bordoni, F. Pacor)*” for the characterization of sites of the Italian National Seismic Network (RSN) with accelerometers.

Here the results for station IV-ROM9 are presented.

Geophysical measurements are two 2D arrays of seismic stations in passive configuration. Using surface-wave analysis, we provide results in terms of dispersion curves that are inverted to obtain shear-wave velocity ( $V_s$ ) profiles for the studied area. The inverted models are suitable for computing the average  $V_s$  velocity in the uppermost 30 m ( $V_{s30}$ ) and assegning then the EC8 class.



## 2. Geophysical investigation

Figure 1 shows the location of the seismic stations used for the two 2D array deployed in the target area surrounding IV.ROM9.

IV.ROM9 station is situated in the garden of INGV Rome headquarter.

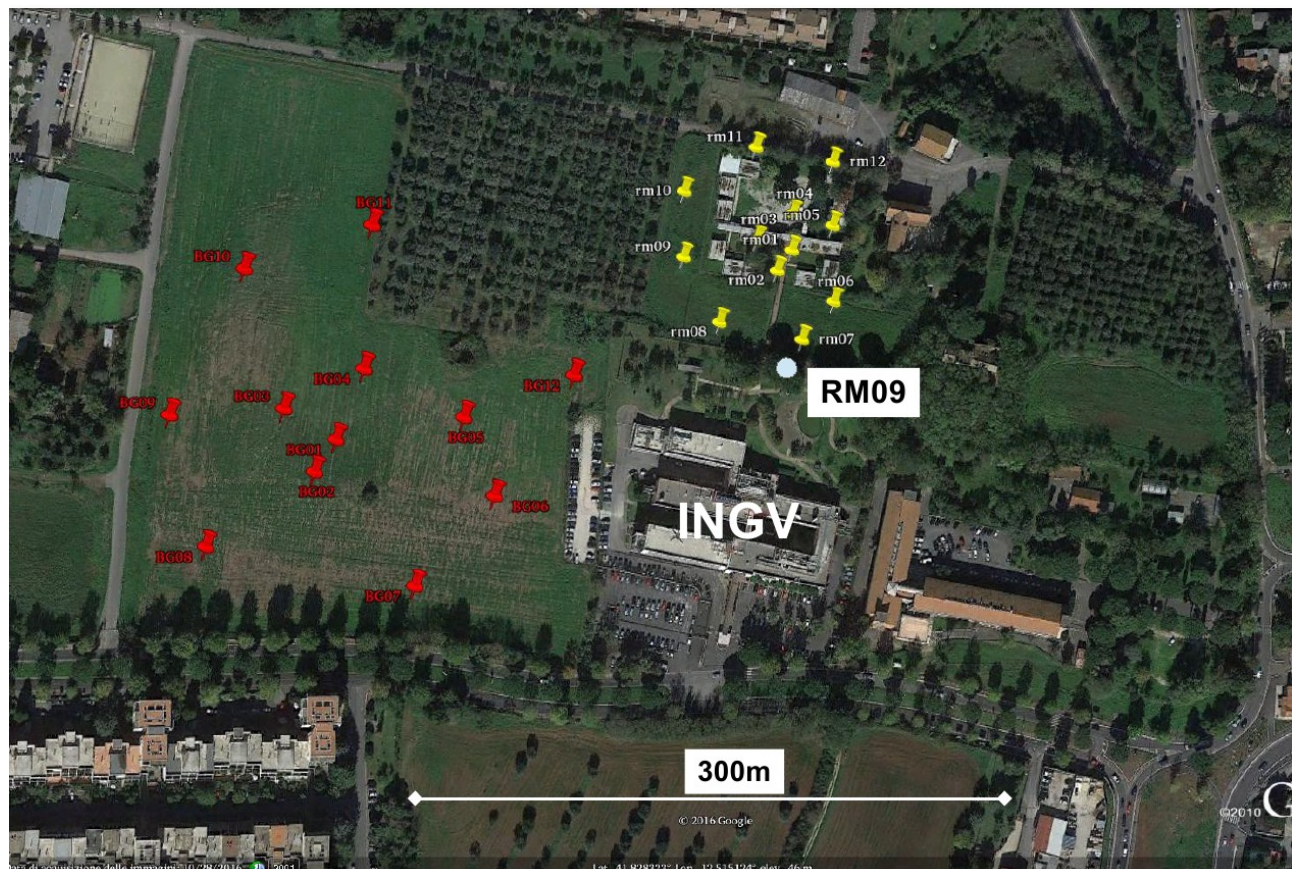


**Figure 1:** Plan view of the two 2D seismic arrays deployed in the area of IV-ROM9 site. The yellow and red points indicate the twelve stations of the 2D array in passive configuration (named “small” and “big” array, respectively). All stations are equipped with Reftek R130 digitizer and Lennartz 3D-5sec velocimetric sensors. The filled circle symbol indicates the position of IV-ROM9 station.

## 2.1 ARRAY MEASUREMENTS RESULTS

Two 2D arrays were performed using 12 single seismic stations equipped with Reftek 130 digitizers and Lennartz 3d-5s velocimetric sensors. Figure 1 shows their position, and hereinafter we referred to these two arrays as “big” and “small” array. The common noise recording lasted approximately 2 and 3 hours for the *small* and *big* array, respectively. The measurements were recorded the 9th of March 2017 for the *small* array (maximum aperture 97 m), and the 10th of March 2017 for the *big* array (maximum aperture 205 m). A view of field work is shown in Figure 2. The seismic sensors were positioned in a two-dimensional geometry with irregular spacing, as shown in Figure 2.

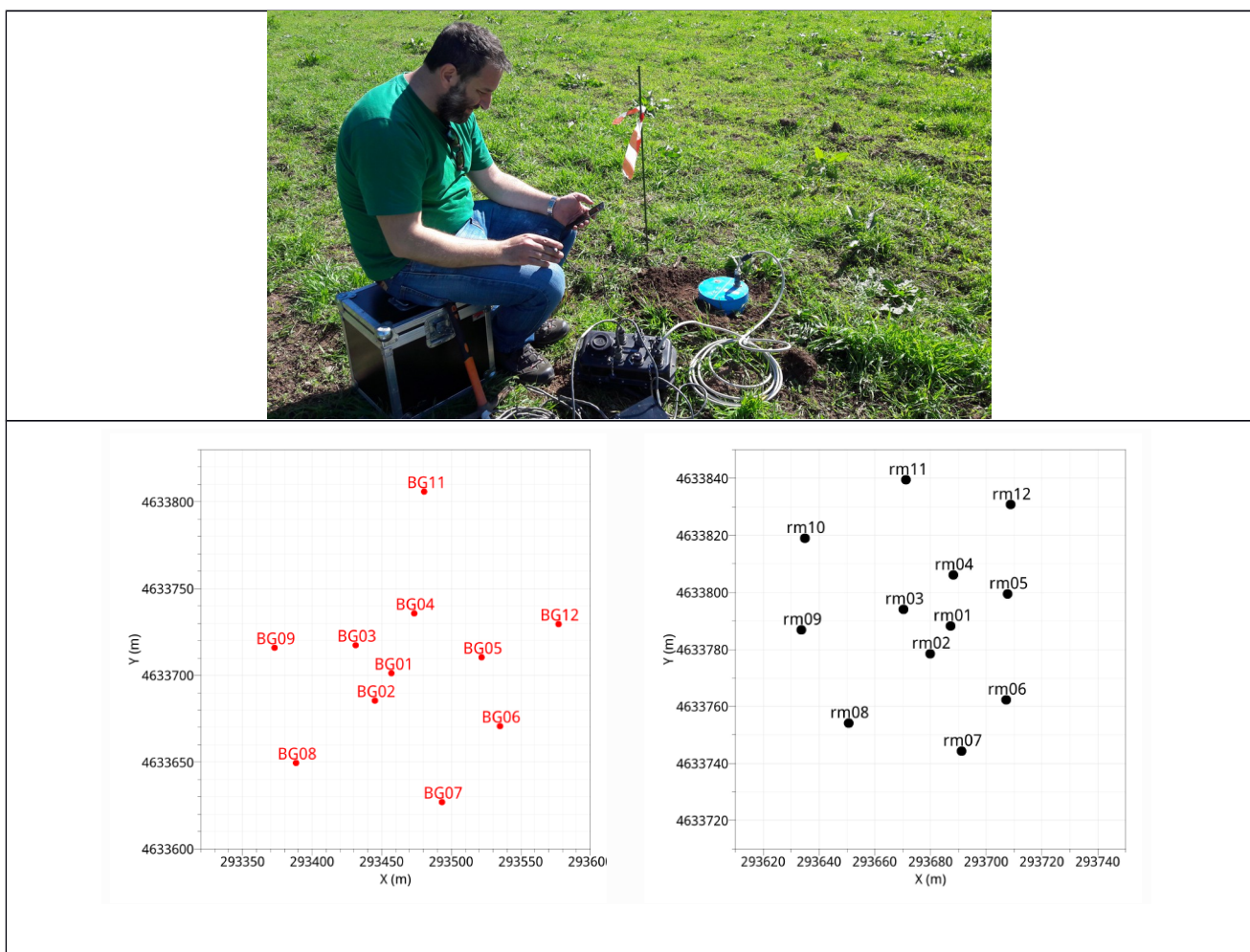


**Figure 2:** Top: Example of an installation of a seismic station. Bottom: 2D Array geometry of the *big* (left panel) and *small* (right panel) array.

The geometry of the array allows the performance in terms of wavenumbers described in Figure 3, where the theoretical Array Transfer Function is reported for each array.

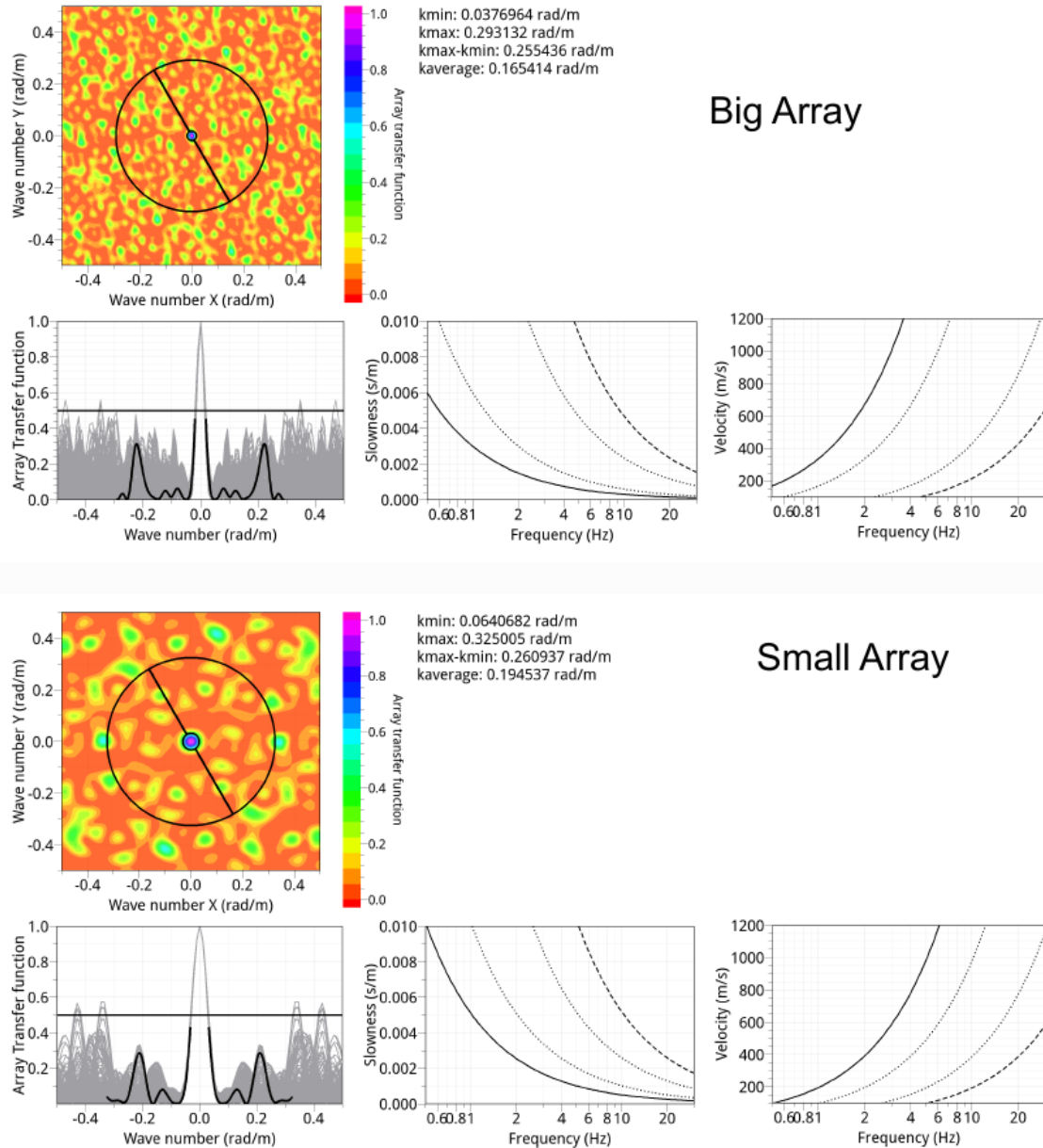


**Figure 3: Theoretical Array Transfer function of the two 2D arrays installed in the target area of IV-ROM9.**

The computed H/V curves of the 12 stations are overimposed at each array in Figure 4. There is a good agreement for the H/V curves showing a good overlapping between 0.4-7 Hz. The resonance frequency ( $F_0$ ) is observed at 1 Hz. The rotated HV spectral ratios also show consistency among the stations of the array, with no significant polarization effects around  $F_0$  (Figure 5 where we show for semplicity only the results of the *small* array).

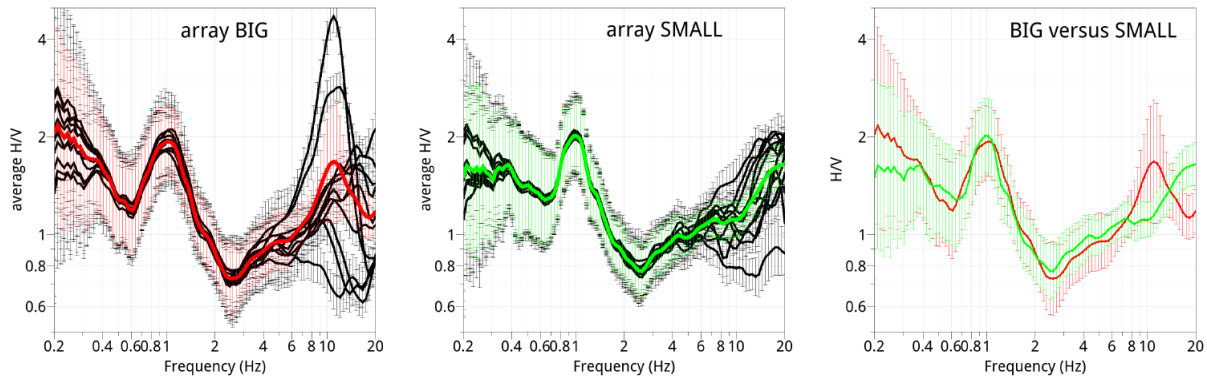


**Figure 4:** H/V curves of the 12 stations for the **big** (left panel) and **small** array (middle panel). The red and green curves are the average H/V curves at these two arrays, and are compared in the right panel. The vertical bars estimate the H/V uncertainty.

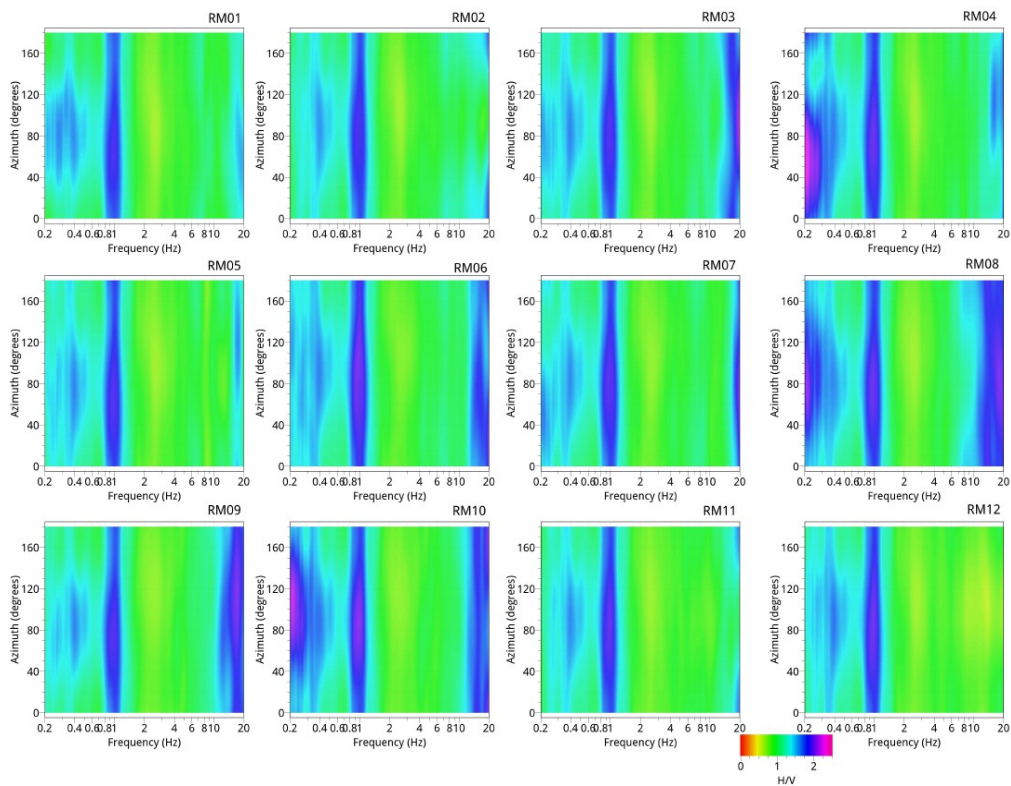


**Figure 5:** Rotating H/V curves at the 12 stations of the **small** array..

Data from the 2D arrays have been analysed in terms of conventional frequency-wavenumber (FK) analysis and high-resolution FK analysis. Because the two techniques lead to similar results, we present hereinafter only the results of the conventional FK method. Although the FK analysis was performed on the three-components of motion, we refer for semplicity only to the records of the vertical component. We used the GEOPSY code (<http://www.geopsy.org>) for the H/V computation and surface-wave analysis. In Figure 6 the dispersion curve is shown.

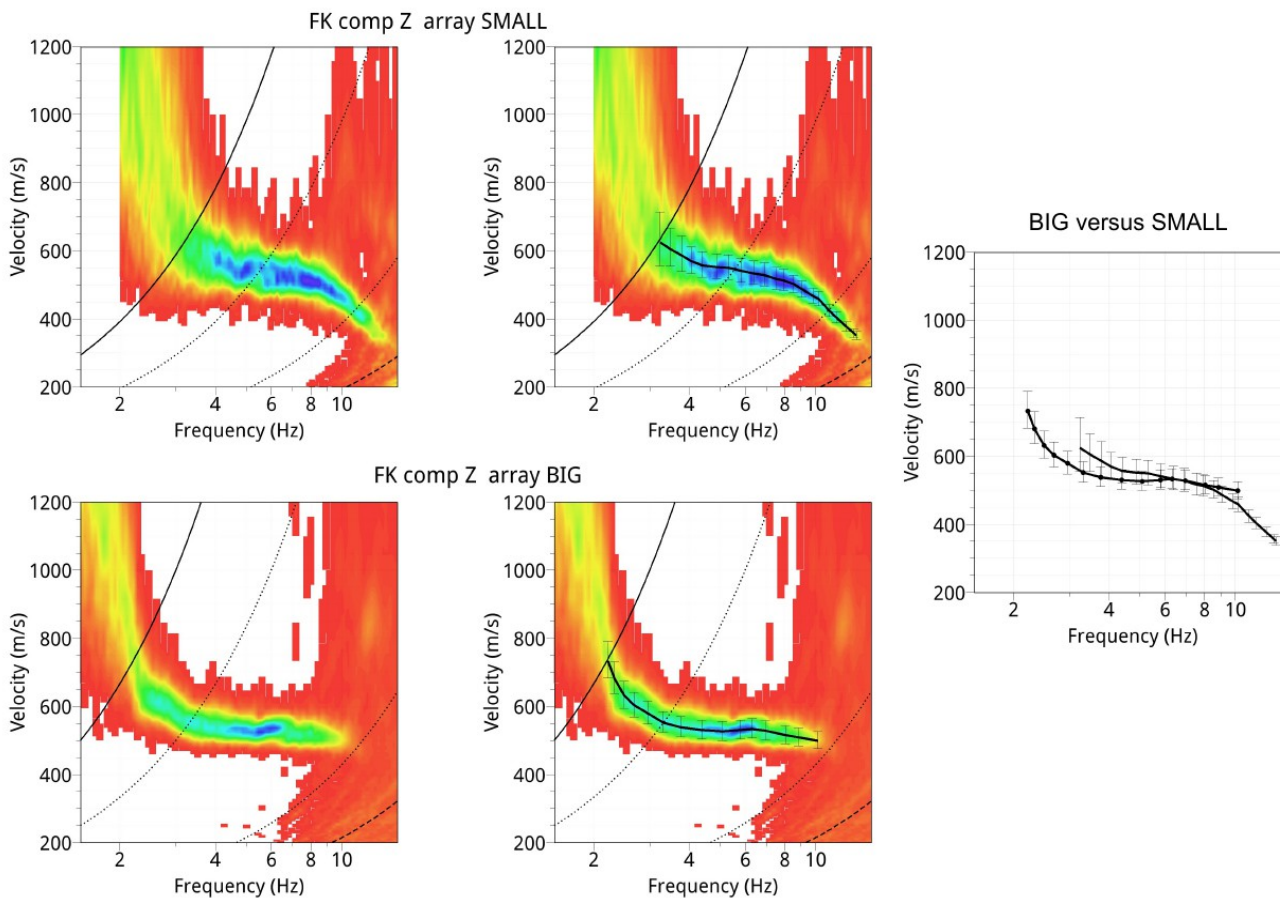


**Figure 6:** Unpicked and picked dispersion curve in the velocity-frequency plan for the *small* (top) and *big* array (bottom panel). On the right, the picked dispersion curves derived from the two arrays are overimposed.

The modified spatial auto-correlation technique (MSPAC) was also applied to the passive data to obtain the auto-correlation curves (Figure 7).

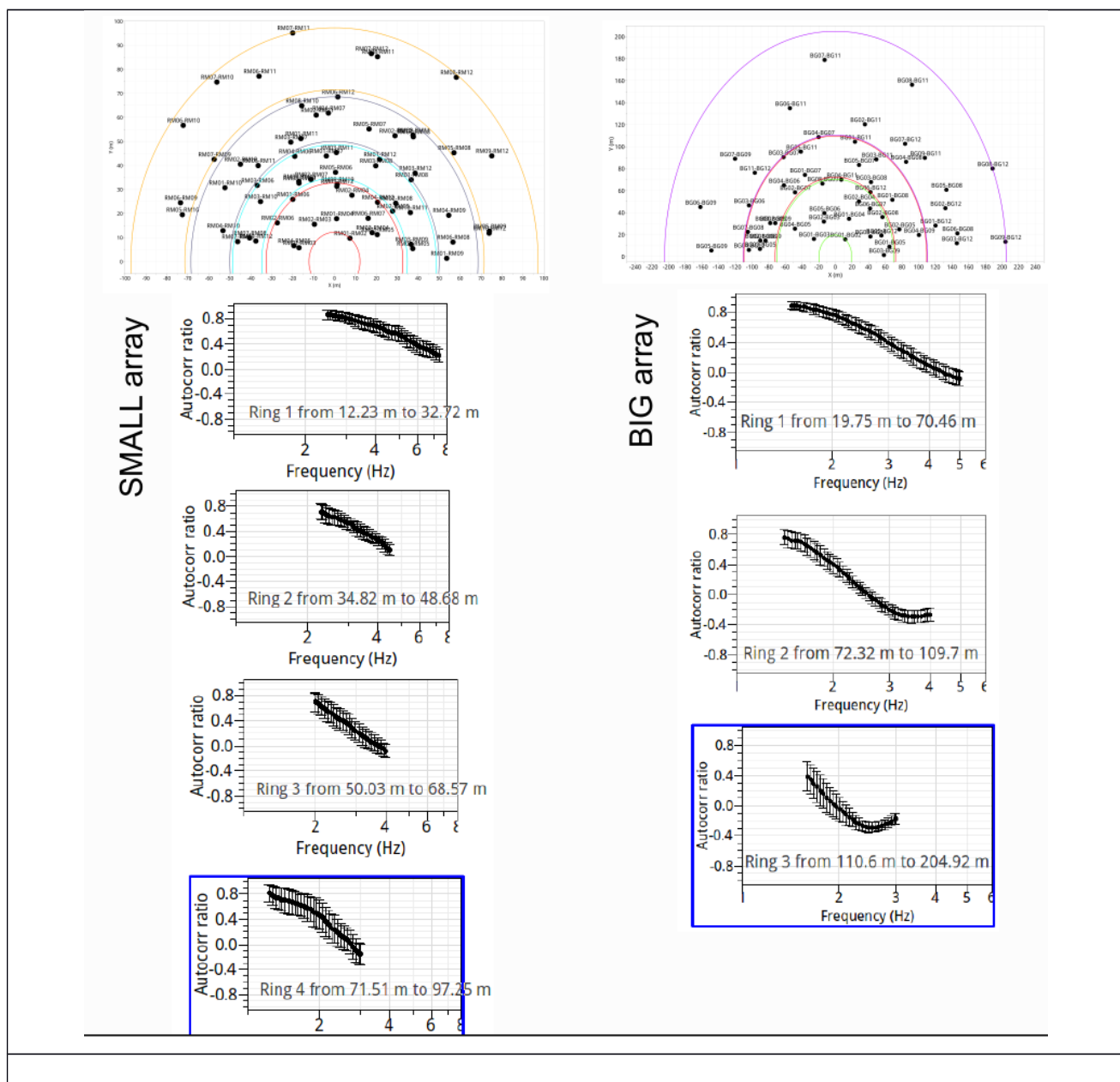


**Figure 7: MSPAC analysis showing the selected rings and the corresponding autocorrelation curves for the small (left) and big array (right panel).**

### 3. Vs Model

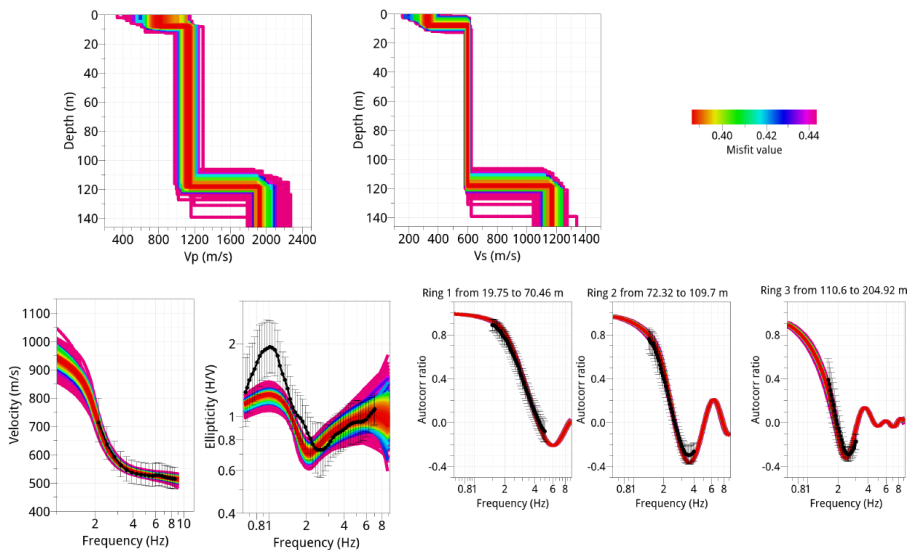
Comparing the dispersion curves coming from the two arrays (Figure 6), we observe that they are almost aligned in the common frequency band. As first approximation, we do not merge the two dispersion curves obtained from *big* and *small* array, but we keep them separated. To proceed with the inversion, we assume that the dispersion curve derived from the vertical component of motion was the fundamental mode of Rayleigh waves.

Moreover, we insert the additional targets during the inversion process:

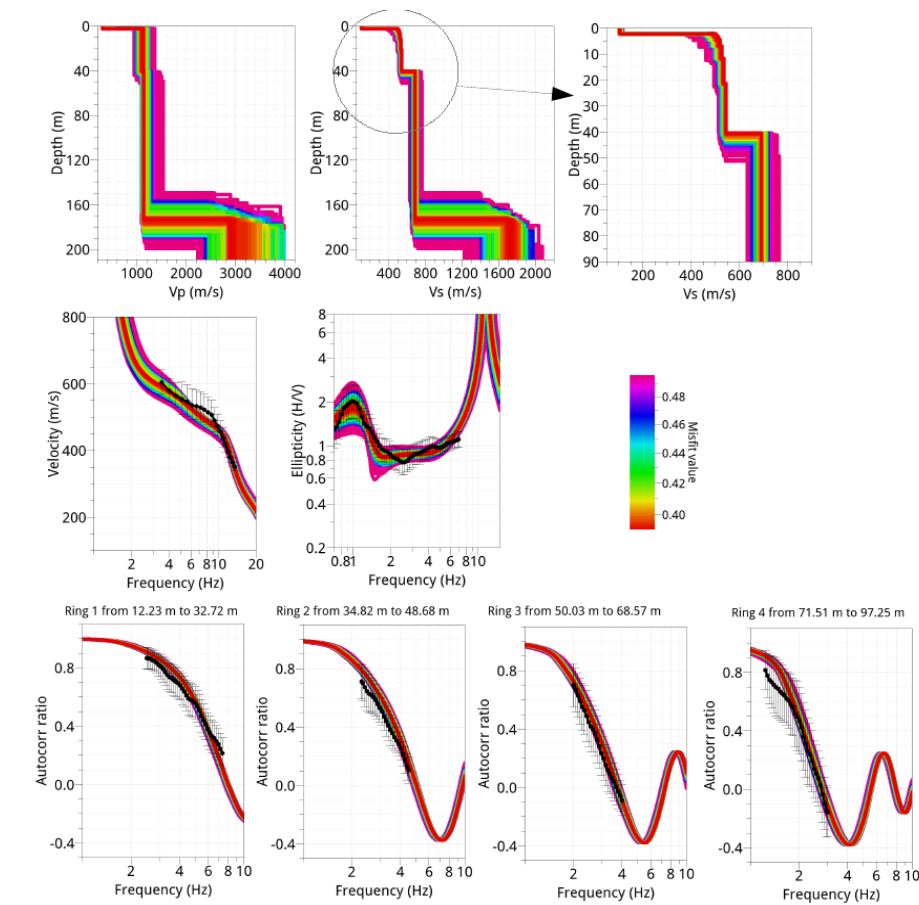
- 1) Ellipticity curve selected in the most common part (from 0.7 to 7 Hz; see Figure 4)
- 2) Fundamental frequency ( $F_0=1$  Hz)
- 3) Autocorrelation curves obtained by MSPAC analysis (Figure 7).

Figure 8 shows for the *big* array the comparison between the targets obtained experimentally and the ones expected for the velocity ( $V_p$  and  $V_s$ ) models, using a very simple model parameterization composed of two main layers over halfspace. Focusing on the best  $V_s$  models (i.e. lowest misfit) of Figure 8, the results indicate a very uppermost first layer (thickness < 10 m) with  $V_s$  around 300-350 m/s, whereas the second layer show a  $V_s$  of about 600 m/s. The halfspace is obtained from the inversion at about 110-140 m of depth.

The resulting models for the *small* array are shown in Figure 9. Here we refined the parameterization of the second layer, allowing a shear-wave velocity increasing with depth. In this inversion, a seismic contrast is found at a depth from 40 to 50 m (Figure 9).



**Figure 8:** Resulting models obtained at the **big 2D array**. The inversion procedure constrained the dispersion curves, the H/V curve as well as with the MSPAC autocorrelation analysis (the field data are shown as black curves).



**Figure 9:** Resulting models obtained at the **small 2D array**. A zoom of Vs profile is also reported for the first 90 m (see the unfilled circle).

The best Vp and Vs model of the *small* array are proposed in Figure 10 and Table 1.

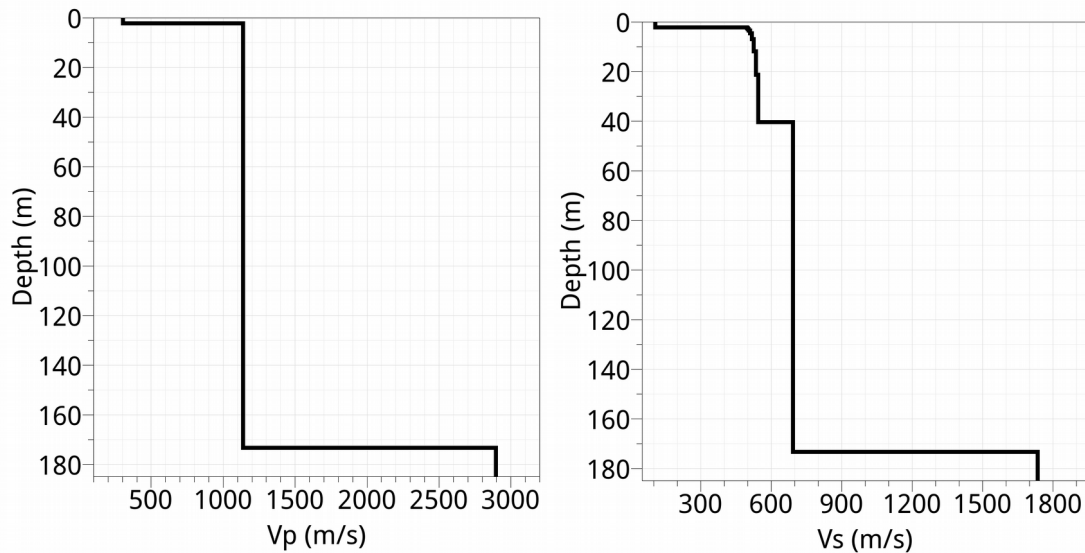


**Figura 10: Best-fit model of  $V_p$  (left panel) and  $V_s$  (right panel) values (small array) [extracted from the ensemble of Fig. 9].**

<b>From (m)</b>	<b>To(m)</b>	<b>Thickness (m)</b>	<b><math>V_s</math> (m/s)</b>	<b><math>V_p</math> (m/s)</b>
0	2,20	2,2	105	303
2,2	40,4	38,2	495-544	1137
40,4	173	132,6	691	1137
173		?	1734	2895

**Table 1: Best-fit model**

#### 4. Conclusions

The H/V analysis of IV.ROM9 site shows a clear resonant peak at 1 Hz, suggesting as order of the bedrock depth 100-200 meters. The very uppermost meters (< 5m) could be linked to the presence of superficial landfill material (Figures 9 and 10). A second layer of about 40-50 m thickness and with average Vs around 500-550 m/s could be related to volcanic materials. Below, a stiffer layer with Vs around 700 m/s could be connected to loose gravels and/or overconsolidated clay. The best models found the seismic bedrock 170 m deep.

The  $V_{s30}$  retrieved from the best inverted model is 410 m/s (Table 2), therefore IV-ROM9 is classified as class B soil type following the NTC08 seismic classification.

$V_{s30}$ (m/s)	<b>Soil class</b>
410	B

Table 2: Soil Class

### ***Disclaimer and limits of use of information***

The INGV, in accordance with the Article 2 of Decree Law 381/1999, carries out seismic and volcanic monitoring of the Italian national territory, providing for the organization of integrated national seismic network and the coordination of local and regional seismic networks as described in the agreement with the Department of Civil Protection.

INGV contributes, within the limits of its skills, to the evaluation of seismic and volcanic hazard in the Country, according to the mode agreed in the ten-year program between INGV and DPC February 2, 2012 (Prot. INGV 2052 of 27/2/2012), and to the activities planned as part of the National Civil Protection System.

In particular, this document<sup>1</sup> has informative purposes concerning the observations and the data collected from the monitoring and observational networks managed by INGV.

INGV provides scientific information using the best scientific knowledge available at the time of the drafting of the documents produced; However, due to the complexity of natural phenomena in question, nothing can be blamed to INGV about the possible incompleteness and uncertainty of the reported data.

INGV is not responsible for any use, even partial, of the contents of this document by third parties and any damage caused to third parties resulting from its use.

The data contained in this document is the property of the INGV.



This document is licensed under License

Attribution – No derivatives 4.0 International (CC BY-ND 4.0)

---

<sup>1</sup>This document is level 3 as defined in the "Principi della politica dei dati dell'INGV (D.P. n. 200 del 26.04.2016)"

### ***Esclusione di responsabilità e limiti di uso delle informazioni***

L'INGV, in ottemperanza a quanto disposto dall'Art.2 del D.L. 381/1999, svolge funzioni di sorveglianza sismica e vulcanica del territorio nazionale, provvedendo all'organizzazione della rete sismica nazionale integrata e al coordinamento delle reti sismiche regionali e locali in regime di convenzione con il Dipartimento della Protezione Civile.

L'INGV concorre, nei limiti delle proprie competenze inerenti la valutazione della Pericolosità sismica e vulcanica nel territorio nazionale e secondo le modalità concordate dall'Accordo di programma decennale stipulato tra lo stesso INGV e il DPC in data 2 febbraio 2012 (Prot. INGV 2052 del 27/2/2012), alle attività previste nell'ambito del Sistema Nazionale di Protezione Civile.

In particolare, questo documento<sup>1</sup> ha finalità informative circa le osservazioni e i dati acquisiti dalle Reti di monitoraggio e osservative gestite dall'INGV.

L'INGV fornisce informazioni scientifiche utilizzando le migliori conoscenze scientifiche disponibili al momento della stesura dei documenti prodotti; tuttavia, in conseguenza della complessità dei fenomeni naturali in oggetto, nulla può essere imputato all'INGV circa l'eventuale incompletezza ed incertezza dei dati riportati.

L'INGV non è responsabile dell'utilizzo, anche parziale, dei contenuti di questo documento da parte di terzi e di eventuali danni arrecati a terzi derivanti dal suo utilizzo.

La proprietà dei dati contenuti in questo documento è dell'INGV.



Quest'opera è distribuita con Licenza

Creative Commons Attribuzione - Non opere derivate 4.0 Internazionale.

---

<sup>1</sup>Questo documento rientra nella categoria di livello 3 come definita nei "Principi della politica dei dati dell'INGV (D.P. n. 200 del 26.04.2016)".